

SOOT FILTRATION SIMULATION – GENERATION OF POROUS MEDIA ON THE MICRO SCALE FROM SOOT DEPOSITION ON THE NANO SCALE

Andreas Wiegmann

Fraunhofer Institut für Techno- und Wirtschaftsmathematik,
Fraunhofer Platz 1, 67663 Kaiserslautern, Germany.
Tel.: +49 631 31600 4380
Fax: +49 631 31600 5380
E-mail: wiegmann@itwm.fraunhofer.de

Stefan Rief

Fraunhofer Institut für Techno- und Wirtschaftsmathematik,
Fraunhofer Platz 1, 67663 Kaiserslautern, Germany.
Tel.: +49 631 31600 4558
Fax: +49 631 31600 5558
E-mail: rief@itwm.fraunhofer.de

Arnulf Latz

Fraunhofer Institut für Techno- und Wirtschaftsmathematik,
Fraunhofer Platz 1, 67663 Kaiserslautern, Germany.
Tel.: +49 631 31600 4301
Fax: +49 631 31600 5301
E-mail: latz@itwm.fraunhofer.de

Abstract :

In soot filtration simulation, there exists a discrepancy of scales. The filter media can be represented with a resolution of a micron, while the soot particles can be as small as 20 nanometers. A representative portion of the media is needed, but also the correct deposition behavior of the soot particles in order to achieve realistic clogging behavior.

A hierarchy of simulations may help with this. On the nanometer scale, at 10 nanometer resolution, a three-dimensional computer model of 4^3 microns of the filter media geometry is built. With this resolution, soot particles are well resolved, and collisions with walls and other particles are explicitly those of solid bodies. When significant amounts of particles have been deposited, a porous region has grown near the solid parts of the model. The exact nature of this region depends on the process parameters, and the method allows also keeping track of the dynamics of this buildup of the porous media. After this step, a second simulation is run on the micro scale. Now, as much as a cubic millimeter of the filter media is represented in the computer, with a resolution of about two microns. The porous structure from the nanometer scale simulation now shows as cells that are neither empty nor solid, but rather porous cells. Changes of porosity and permeability on the micro scale are governed by the precise information from the nanometer scale simulations, and are used on the micro scale to eventually predict effects like filter efficiencies and filter life time, that can be measured for the real filter media.

Key words: nanometer scale deposition simulation, filter efficiency simulation, filter lifetime simulation

1. Introduction

The filter media is arguably the most important factor in filtration applications. Sophisticated and geometrically complex materials are in use, yet still little is understood how they actually work or do not work. Many academic groups and engineers in filter companies study filtration using commercial simulation approaches on the macroscopic or filter scale, see [1,2]. Our own work

has been on simulating the filtration effects in the filter media, on the fiber scale or pore scale [3,4]. At the same time, simulation became useful for the study of the lowest scale effects, particles depositing on single fibers [5]. The present work is interested in providing a step towards connecting these two scales. In Diesel Particulate Filtration, the soot particles are 2-3 orders of magnitude smaller than the structures and pores of the ceramic filter, at 20-100 nm particle diameter compared to about 10-20 μm pore diameters. Current desktop computer models are capable of handling about 500^3 cells, which means $5^3 \mu\text{m}^3$ at a resolution of 10 nm, the minimum if soot particles are to be resolved. Thus, not a single pore would be covered by such simulation. Yet the pores partial obstruction by a porous layer of deposited soot is the main mode of operation of diesel particulate filtration. To overcome this discrepancy of scales, or simulation gap, the concept of porous besides filled and empty computational cells is added to our models [3,4]. Only with this addition, the complex pore structure and variations of grain sizes in sintered materials, etc., can be accounted for in the simulation.

The following paragraphs detail our approach how to establish the needed parameters for this new type of cell, namely the permeability and clogging mechanisms. But first the stage is set by describing the ceramic model, the soot model and the resolved computations on the nanometer scale. All geometric modeling, flow and filtration simulation was performed with the **GeoDict** Software's **NONWOVEN**, **PoroDict** and **FilterDict** modules. See <http://www.geodict.com>.

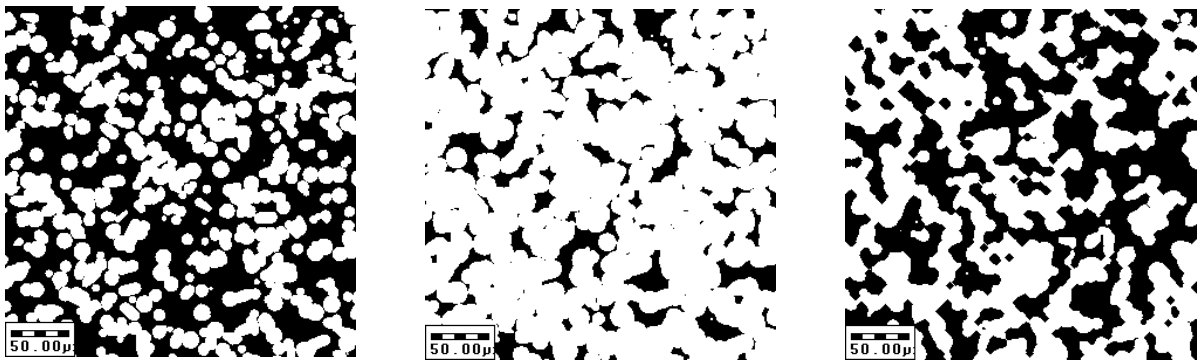


Figure 1: a) Two-dimensional cross section view of randomly placed overlapping spheres and short fibers (white). The porosity is about 65 %. b) View of the same slice after dilation with 3 voxels is applied to the data. c) Same slice as in Figure a and b, after dilations of 2 voxels and 1 voxel are applied. The porosity is about 45 %.

2. Ceramic model for a diesel particulate filter

The current three-dimensional ceramics model is based on an earlier three dimensional nonwoven model [6]. By setting the fiber length to zero and choosing spherical fiber ends, fibers become spherical particles. Such spherical particles are placed at random locations in the computational domain, a parallelepiped of n_x by n_y by n_z cubical computational cells that we refer to as voxels, or volume elements, after the two-dimensional word pixel, or picture elements. The resolution, or cell width, is on the order of 1 μm . A selection of spherical and “short fibers” representing non-spherical grains with dimensions around 10 – 20 μm is used (Fig.1a). They are allowed to overlap in the generation process, and we stop inserting new particles when a porosity slightly lower than the porosity of the real media is reached. It is well known that so-called morphological operations can be used to model sinter necks in such generated ceramics [7]. We implement this by dilating the grain portion of the three-dimensional image by about 20% (Fig.1b) and then eroding about

15% (Fig. 2). The precise values of all these parameters need to be found by iterating the procedure, until satisfactory agreement with the real media is reached.

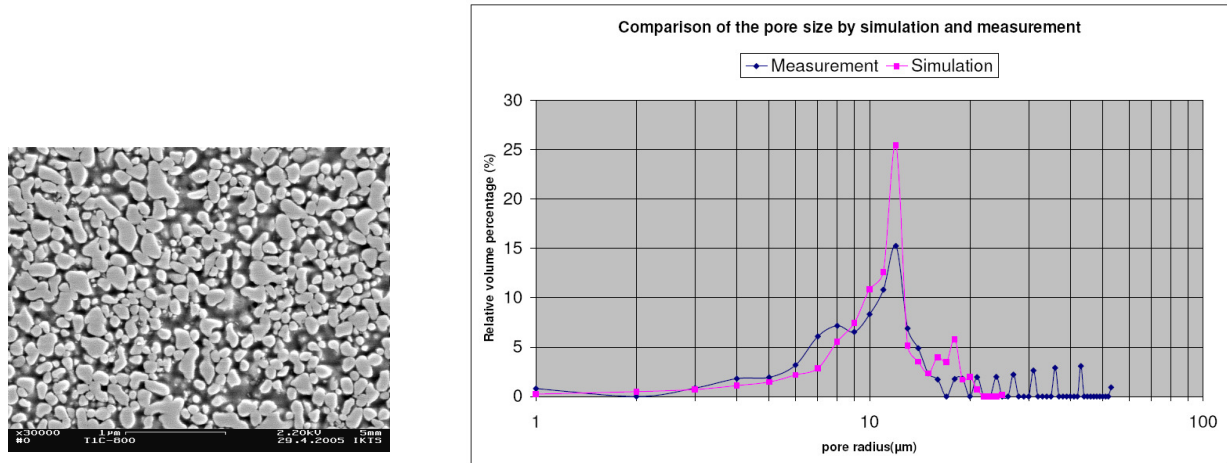


Figure 2: a) *Raster Electron Microscopy image of an Al_2O_3 ceramic (Courtesy Dr. Krell, Fraunhofer IKTS). Besides the different scale, a higher solid volume fraction and smaller sinter necks are easily visible to the human eye. Such comparisons are the first step to find the correct parameters for the material models. B) Pore-size measurements by the mercury intrusion method in dark blue vs. the computed pore size distribution of a media model of the same material in pink. The media was described by a frequency distribution of 20 fiber types. The discrepancy for large pore sizes bigger than $30\ \mu\text{m}$ is still under investigation, and is currently considered an artefact of the experimental method.*

3. Validation of the ceramic model

Media models must be based on “real” input quantities that media developers think in. Examples are porosity, fiber diameters and fiber anisotropy for nonwoven, or pore size distributions, media thickness, specific surface area, etc., to name but a few. Currently, these are not the input parameters for the computer model in §2, and so a loop of media generation and media inspection is necessary that we hope to cut out in the future. The three means of validation are: first, comparison between real and generated media by a human. While this can not ensure validity of the model, it detects obvious problems. Figures 1 c) and 2 a) illustrate the input data for this mode of validation. The second, more sophisticated way of validation is the comparison of two-dimensional and three-dimensional image measures of real and generated media, such as the chord length distribution, if microscopic or tomographic representations of the media are available. More complex are comparisons of simulated Porometry, Mercury Porosimetry or challenge tests with measurements, and finally the third means of validation are comparisons of filter efficiency or filter life time simulations with measurements. Such comparisons are currently carried out and will be reported in the future. For now, Figure 2 b) serves to illustrate as an example how measured and simulated Mercury Porosimetry may compare rather well.

4. Soot model, particle transport and collision model

Real soot particles have highly complex shapes as agglomerates of smaller particles. This complexity is not accounted for in our model. For the purpose of the collision simulation we assume spherical particles with diameter similar to that of the agglomerates. For the transport

portion, we assign a lower density that accounts for the “porous” structure of these spherical particles. Soot particles are assumed to stick to any surface of the ceramics or previously deposited soot that they touch. Two effects contributing to the particle velocity are friction and diffusion. Equations (1) give the precise formulation for the particle transport except for collisions. Particles can be positioned anywhere in space, while the fluid velocity is only available at the centers of the computational cells. To approximate fluid velocities at the particle location, these discrete velocity values are linearly interpolated.

$$\begin{aligned} \frac{d\vec{v}}{dt} &= -\gamma \times (\vec{v}(\vec{x}) - \vec{v}_o(\vec{x})) + \frac{Q\vec{E}_o(\vec{x})}{m} + \sigma \times \frac{d\vec{W}(t)}{dt} \\ \frac{d\vec{x}}{dt} &= \vec{v} \\ \gamma &= 6\pi\rho\mu\frac{R}{m} \\ \sigma^2 &= \frac{2k_B T\gamma}{m} \\ \langle dW_i(t), dW_j(t) \rangle &= \delta_{ij}dt \end{aligned}$$

t :	time
\vec{x} :	particle position
\vec{v} :	particle velocity
R :	particle radius
m :	particle mass
Q :	particle charge
T :	ambient temperature
k_B :	Boltzmann constant
$d\vec{W}(t)$:	3d probability (Wiener) measure
\vec{E}_o :	electric field
\vec{v}_o :	fluid velocity
ρ :	fluid density
μ :	fluid viscosity

Equations (1). *Lagrangian description of particle motion.*

Because particles are spherical, only the distance of the particle center from the nearest obstacle determines collisions. As soon as the particle center is found nearer to a ceramic voxel or previously deposited soot particle, the particle is considered as filtered. This is done in two different ways. In the resolved computations, particles are bigger than voxels, and are converted into solid voxels themselves. In the under-resolved computations, particles are much smaller than voxels, and are entered as additional mass into the newly introduced porous voxels. Porous voxels can fill up with soot only up to a previously determined porosity. The details of this procedure are now given.

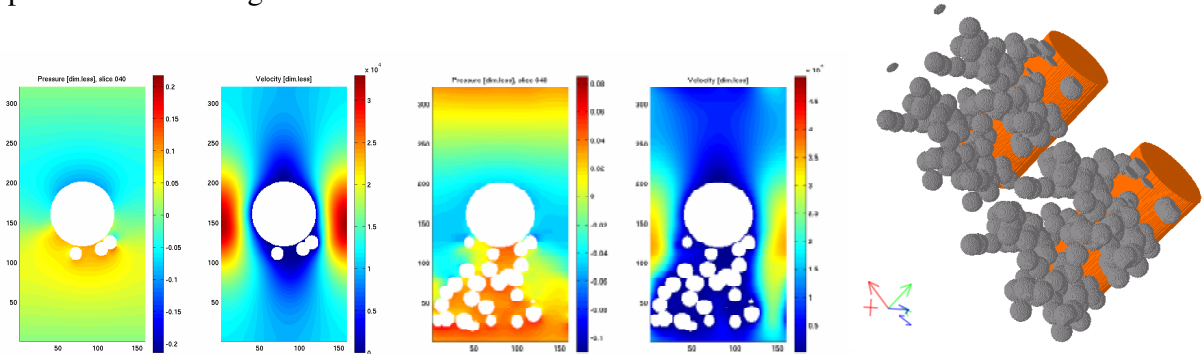


Figure 3: a) Pressure and b) magnitude of velocity of flow around a fiber with few deposited particles. c) Pressure and d) magnitude of velocity of flow around a fiber with more deposited particles. e) 3-dimensional view of the fiber and deposited particles in c) and d), with additional copies of the domain to illustrate the periodic boundary conditions.

5. Nanometer scale fully resolved simulation

In the slow flows occurring in soot filtration, the Stokes equations describe the motion of air through the pores. The pressure difference, together with the media model, provides the needed boundary conditions. We assign no-slip on the surfaces of the ceramic voxels. The pressure difference is converted into a driving volume force, and periodic boundary conditions are used on the boundaries of the computational domain. Equations (2) are the Stokes-Brinkmann equations that include a Darcy-type permeability κ in addition to the usual Stokes equations. In the empty voxels, you can think of κ as infinity, and the additional term simply drops out. The nanometer scale computations alternate between the partial differential equations (2) and the stochastic ordinary differential equations (1). First, equations (2) are solved in the empty ceramics. Then, a predetermined number of soot particles are moved according to equations (1) until they stick to a surface or leave the computational domain.

$$\begin{aligned} -\mu\Delta\vec{u} + \kappa^{-1}\vec{u} + \nabla p &= \vec{f} \text{ (momentum balance)} \\ \nabla \cdot \vec{u} &= 0 \text{ (mass conservation)} \\ \vec{u} &= 0 \text{ on } \Gamma \text{ (no-slip on solid surfaces)} \end{aligned}$$

$$\begin{aligned} \vec{f} = (0, 0, f) &: \text{ force in flow}(z)\text{-direction,} \\ \kappa &: \text{ porous voxel permeability,} \\ \vec{u} &: \text{ velocity,} \\ \mu &: \text{ fluid viscosity,} \\ p &: \text{ pressure and} \\ \Gamma &: \text{ surfaces of ceramic or deposited particles.} \end{aligned}$$

Equations (2). Stokes-Brinkmann equations and notation.

Now, the deposited particles obstruct the flow of air, and the procedure repeats with equations (2), but now in the new structure consisting of the original ceramic and deposited particles. Figure 3 shows a cross section of pressure and velocities around a single fiber. In a) and b), only a few particles have deposited on the fiber, in c) and d) a porous layer of deposited particles has formed. Not shown are 8 intermediate geometries for which the flow is also computed. Figure 3 e) shows 4 copies of the 3-dimensional computational domain from Figure 3 c) and d) in order to illustrate the meaning of the periodic boundary conditions in the lateral directions. The flow “feels” the “neighboring fibers”, and sees an “infinitely long” fiber.

6. Micro scale under-resolved simulation

The computations in §5 can be carried out for many sets of process parameters: different mean velocities, different particle size distributions, different particle densities, etc. It can be seen from Figure 3 e) that after some time new particles deposit only on top of a porous layer or cake which they can not enter because the pores are too small. For the micro scale, the porosity and permeability of these layers in dependence of the process parameters must be evaluated. However, this approach only finds the values for the cake after it is formed. During the simulation, also the forming of this cake must be accounted for. So, we denote the final cake parameters by permeability κ_{\min} and solid volume fraction s_{\max} . Observing that for small solid

volume fraction and slow flows, the flow resistivity $\sigma = \kappa^{-1} \mu$ depends linearly on the solid volume fraction s , we propose the definition of local permeability κ via the formula given in equation (3).

$$\kappa = \kappa_{min} \cdot \max \left(1, \frac{s_{max}}{s} \right)$$

Equation (3). Definition of flow permeability κ in dependence of local solid volume fraction s .

The micrometer scale computations also alternate between the partial differential equations (2) and the stochastic ordinary differential equations (1). First, equations (2) are solved in the empty ceramics. Then, a predetermined number of soot particles are moved according to equations (1) until they stick to a surface or leave the computational domain. One difference is that on the micrometer scale many more particles are moved with the same velocity field, as the influence per particle is much smaller on this scale. Now the particles can not be entered as solid voxels as in the nanometer scale case. Instead, we keep track of the amount of mass that enters into a voxel. When all particles of this first stage have been either deposited in one of the empty voxels or have moved out of the computational domain, the structure is reprocessed. For all voxels where particles have entered, the local porosity is updated according to the amount of mass that has entered. Then, the local permeability is found using equation (3) and the relation between flow resistivity and permeability. Finally, voxels are marked as impermeable where the solid volume fraction is larger than s_{max} . This means that in the next run particles will deposit on their surface rather than enter them. Now the loop is complete, the flow field is recalculated, albeit this time with some nontrivial values of κ for those voxels where particles have deposited in the previous runs.

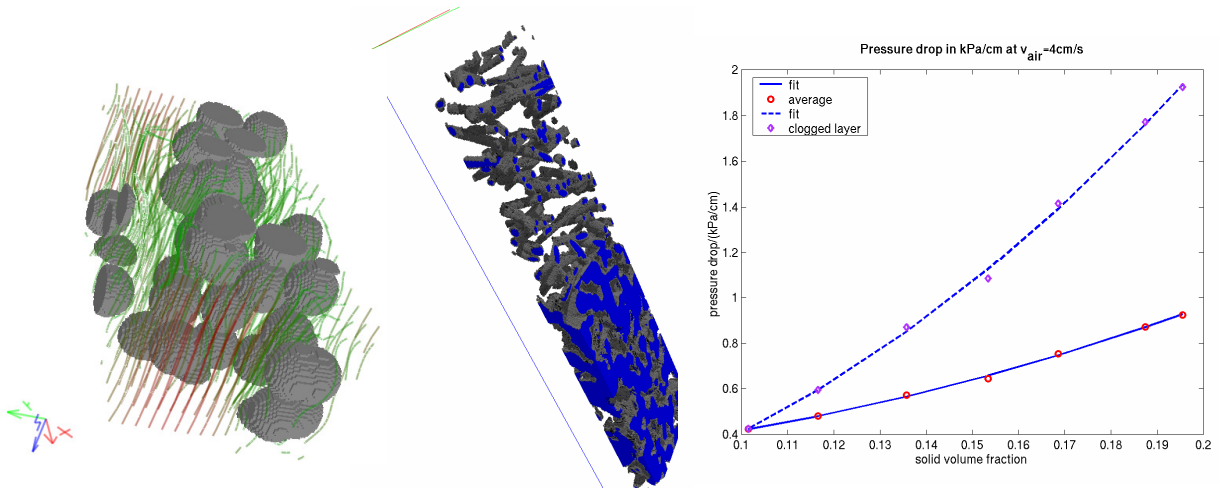


Figure 4: a) Layer of deposited particles from nanometer scale computation. The stream lines illustrate that local flow properties are evaluated to find the permeability. b) A cutout of a three dimensional 2-layered filter media. The media is in blue, different densities of deposited soot are indicated by different shades of grey. c) Illustration of overall pressure drop and local pressure drop in clogged area. The simulation indicates that not all parts of the media work equally hard.

7. Results

Putting the nanometer scale simulations and micrometer scale together, and running the models for several weeks on a small cluster computer results in clogged filter media as seen in Figure 4 b). First, nanometer scale simulations are run for the flow velocities and particles sizes under consideration. Then, several hundred alternations of solving equations (2) and equations (1) lead to a complex, highly porous structure. Now the solution of equation (2) is scaled so that a given far-field velocity is attained, and thus a pressure drop is computed for every intermediate geometry. A possible behavior of pressure drop is shown in Figure 4 c). Here, both the overall pressure drop and a local pressure drop, over a clogged area, are shown. The rescaling to a given far-field velocity is particularly simply for the Stokes-Brinkmann equations: due to the linearity one simply multiplies the velocities and pressure with an appropriate factor so that the average velocity has the desired value. Further comparisons of simulation results with experiments can unfortunately not be shown due to secrecy agreements, but they are quite promising.

8. Conclusions

We have presented some thoughts, models and equations on how to find the needed local coefficients for micrometer scale filtration simulations from highly resolved nanometer scale simulations. A simple linear interpolation formula equation (3) provides the permeability until a porous voxel is so clogged that no more soot particles can enter. Analyzing in detail the soot distribution in the three-dimensional pores of the filter media will give exciting insights into the possibility of designing new filter media in ongoing and future work. On the other hand, much collaboration with experimenters and simulators from industry and academia must still happen in order to fully realize the potential of the proposed technology.

References

- [1] W. Heikamp and A. Stephan, "Simulation of Oil Saturation in Porous Media", AFS Annual Conference, New Orleans, April 2004.
- [2] N.S. Hanspal, W. R. Ruziwa, V. Nassehi, R.J. Wakeman, "Finite Element Modelling of Flow of Non-Newtonian Fluids in Pleated Cartridge Filters", AFS Annual Conference, New Orleans, April 2004.
- [3] A. Latz and A. Wiegmann, "Simulation of fluid particle separation in realistic three dimensional fiber structures", Filtech Europa, Düsseldorf, October 2003.
- [4] S. Rief, A. Latz and A. Wiegmann, "Research Note: Computer simulation of Air Filtration including electric surface charges in three-dimensional fibrous micro structures", Filtration, Vol. 6 No. 2, 2006.
- [5] M.J. Lehmann and G. Kasper., "Morphology of particulate structures on a dust loaded single fiber: A simulation", Filtech Europa, Düsseldorf, October 2001.
- [6] K. Schladitz, S. Peters, D. Reinel-Bitzer, A. Wiegmann, J. Ohser, "Design of acoustic trim based on geometric modeling and flow simulation for nonwoven", ITWM Technical Report Nr. 72, January 2005. Accepted in Computational Material Science.
- [7] J. Ohser and F. Mücklich, "Statistical Analysis of Microstructures in Materials Science", John Wiley & Sons (2000).
- [8] R.C. Brown, "Air Filtration, An Integrated Approach to the Theory and Application of Fibrous Filters", Pergamon Press, Oxford (1993).